Available online at www.sciencedirect.com

SciVerse ScienceDirect

Physics Procedia 36 (2012) 1498 – 1503

Physics Procedia

Superconductivity Centennial Conference

The influence of $CuFe_2O_4$ nanoparticles on superconductivity of MgB_2

Nikolina Novosel[a], Damir Pajić[a], Željko Skoko[a], Mislav Mustapić[a], Emil Babić[a], Krešo Zadro[a], Joseph Horvat[b]

[a]*Department of Physics, Faculty of Science, University of Zagreb, 10000 Zagreb, Croatia*
[b]*Institute for Superconducting and Electronic Materials, University of Wollongong, Wollongong NSW 2522 Australia*

Abstract

The influence of $CuFe_2O_4$ nanoparticle doping on superconducting properties of Fe-sheated MgB_2 wires has been studied. The wires containing 0, 3 and 7.5 wt.% of monodisperse superparamagnetic nanoparticles (~ 7 nm) were sintered at 650°C or 750°C for 1 hour in the pure argon atmosphere. X-ray diffraction patterns of doped samples showed very small maxima corresponding to iron boride and an increase in the fraction of MgO phase indicating some interaction of nanoparticles with Mg and B. Both magnetic and transport measurements (performed in the temperature range 2−42 K and magnetic field up to 16 T) showed strong deterioration of the superconducting properties upon doping with $CuFe_2O_4$. The transition temperatures, T_c, of doped samples decreased for about 1.4 K per wt.% of $CuFe_2O_4$. Also, the irreversibility fields $B_{irr}(T)$ decreased progressively with increasing doping. Accordingly, also the suppression of J_c with magnetic field became stronger. The observed strong deterioration of superconducting properties of MgB_2 wires is at variance with reported enhancement of critical currents at higher temperatures (determined from magnetization) in bulk MgB_2 samples doped with Fe_3O_4 nanoparticles. The probable reason for this discrepancy is briefly discussed.

Keywords: MgB_2, magnetic nanoparticle doping

1. Introduction

MgB_2 is probably the most investigated superconductor in the last decade due to the many properties promising for wide spread applications (for example for magnets for magnetic resonance imaging). Besides relatively high superconducting transition temperature $T_c \cong 39$ K (compared to commercial superconductors NbTi and Nb_3Sn), MgB_2 has simple crystal structure, simple and low cost procedure of preparation of wires (compared to the high-temperature superconductors) and absence of weak links at grain boundaries. From the point of view of fundamental scientific research, MgB_2 is unique example of two gap superconductor, making thus the opportunity to study experimentally the properties of this class of superconductors.

The disadvantage of MgB_2 is the relatively low upper critical field $B_{c2} \sim 18$ T and weak pinning of magnetic vortices leading to rather small irreversibility field $B_{irr}(T)$ and significant decrease of critical current density $J_c(B)$ in applied magnetic field. Furthermore, the MgB_2 bulk samples and wires are usually very porous, which additionaly reduces transport J_c [1].

1875-3892 doi:10.1016/j.phpro.2012.06.121

To make MgB_2 wires suitable for practical applications it is necessary to improve their in-field J_c. To acheive this, large effort was made in recent years to enhance flux pinning in MgB_2, mainly by dopand addition [2, 3]. More recently special concern was given to the magnetic nanoparticle doping and posibility to acheive strong magnetic attraction force between vortices and magnetic napoparticulated dopands which would enhance flux pinning force. Although there are some reports of enhancement of B_{irr} and $J_c(B)$ of MgB_2 doped with magnetic nanoparticles [4, 5, 6, 7], direct evidence of magnetic flux pinning is still lacking. Besides, detrimental influence of magnetic nanoparticle doping is also observed [8, 9, 10].

Recently we started systematic study of the influence of magnetic nanoparticles on electromagnetic properties of MgB_2 wires [10, 11]. Here we present the results of the study of the effects of superparamagnetic $CuFe_2O_4$ nanoparticles on transport properties of Fe-sheated MgB_2 wires. These particles were chosen due to their superparamagnetic behaviour above 50 K [12] (which should prevent their agglomeration during mixing of powders) and still quite high saturation magnetization M_S. Also, the reaction of very small $CuFe_2O_4$ nanoparticles with Mg and B could produce numerous nano-sized pinning centres, like $MgCu_2$, FeB, Fe_2B and MgO and therefore produce additional core pinning of vortices when compared to Fe_3O_4 nanoparticle doping [4]. The advantage of our study in respect to previous studies [4, 5, 6, 7, 8, 9] is also that we performed both magnetic and transport determination of $B_{irr}(T)$ and $J_c(B)$ of our samples (which makes the results unambigous) whereas previous findings were primarily based on magnetic measurements. Our results clearly show that $CuFe_2O_4$ nanoparticle doping of MgB_2 wires has strong detrimental effect on their application oriented properties ($B_{irr}(T)$, $J_c(B)$) and provide no evidence for the achivement of special magnetic pinning of vortices [5]. The preliminary results for MgB_2 doped with 5.3 wt.% Fe_3O_4 nanoparticles (with size similar to tahat used in [4]) agree with those for $CuFe_2O_4$ doped wires and thus do not confirm the enhancement of J_c reported in [4].

2. Experimental

Undoped and doped iron-sheated MgB_2 wires were prepared by the in-situ powder-in-tube method. Powders of magnesium (Mg, 99%) and amorphous boron (B, 99%) were well mixed in mortar. For prepatation of the doped MgB_2 wires superparamagnetic $CuFe_2O_4$ nanoparticles with average size 6.5 ± 1.5 nm were used in doping ratio 3 and 7.5 wt.% which correspond to 0.59 and 1.53 at.%, respectively. Magnetic properties of $CuFe_2O_4$ nanoparticles were determined previously [12] and it was obtained that they show the superparamagnetic behaviour with the blocking temperature $T_B = 50$ K (in applied field 0.03 T), saturation magnetization $M_S(5.5\text{ T}, 5\text{ K}) = 35.6$ emu/g and coercive field $\mu_0 H_C(5\text{ K}) = 0.014$ T. Mixed powders were filled into pure Fe tube of 10 mm and 6.5 mm outer and inner diameter, respectively. The tubes were drawn to the wires of 1.4 mm outer diameter and the superconducting cores of the wires were of diameter 0.8 mm. Finally, the reaction heat treatments were performed at 650°C and 750°C for 60 min in argon atmosphere. Very recently we prepared also wire doped with 5.3 wt.% Fe_3O_4 nanoparticles (average size 25 nm, $T_B = 280$ K, $M_S(5.5\text{ T}, 5\text{ K}) = 58$ emu/g).

Superconducting cores of prepared wires were examined by the X-ray powder diffraction. XRD patterns were taken at room temperature using Philips powder diffractometer, model PW1820 (Cu Kα radiation, graphite monocromator, proportional counter). The diffraction intensity was measured in the angular range $20° \leq 2\theta \leq 70°$. Magnetic hysteresis loops $M(H)$ up to maximum applied field 5.5 T were measured at various temperatures using commercial MPMS5 magnetometer (*Quantum Design*) equiped with SQUID. The resistance $R(T, B)$ of the prepared wires was measured in the temperature range 2 – 40 K in the applied magnetic fields up to 16 T using AC current ($I = 1$ mA, $f = 18.4$ Hz) [13]. The transport critical current density $J_c(B)$ was obtained from $V - I$ dependences measured using the pulse method, at temperatures 5 K and 20 K. Rectangular pulses with 0.5 ms duration and up to 320 A current were used. The samples for transport measurements (1.5 cm long wires) were supplied with two current and four voltage leads. The magnetoresistance and $V-I$ curves of each sample were measured at different sections of the wires to obtain useful informations about homogeneity of the wire. All presented measurements were made on the section of the wire showing the highest B_{irr} and J_c.

3. Results and discussion

All following results were obtained at the samples annealed at 750°C. The results for samples annealed at 650°C are practically the same, but less detailed. XRD patterns of undoped and $CuFe_2O_4$ doped (3 and 7.5 wt.%) MgB_2 samples (Fig. 1) show well developed MgB_2 phase with approximately the same crystallite size ~ 20 nm. Also, considerable amount of MgO phase is detected, which is increasing with the increase in doping level. Besides, for doped samples small peak at $2\theta = 45°$ is observed, which can be attributed to formation of Fe_2B and/or $MgCu_2$ phase. Other diffraction lines of Fe_2B, $CuFe_2O_4$ (= Fe_3O_4) are mainly overlapping with the diffraction lines of the MgO phase (apart from peak around 35.4°) so they can not be identified with certainty. The increase of the amount of the MgO phase and appearance of the peak at $2\theta = 45°$ with the increasing doping level clearly indicate that to some extent the reaction between $CuFe_2O_4$ particles and Mg and B occured during the heat treatment of the wires. This finding is also consistent with the absence of the most intense peak in XRD pattern of $CuFe_2O_4$ nanoparticles (situated around $2\theta = 35.4°$) and with recent Mössbauer results for MgB_2 doped with 20 nm Fe_3O_4 nanoparticles [14] showing no presence of Fe_3O_4 phase.

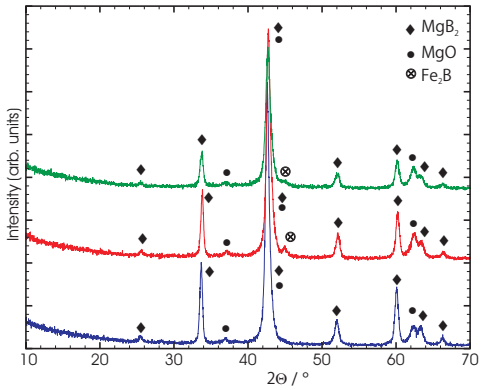

Fig. 1. XRD patterns of $CuFe_2O_4$ doped MgB_2 samples: 0 wt.% (blue), 3 wt.% (red), 7.5 wt.% (green).

Temperature dependences of magnetoresistance of undoped and doped MgB_2/Fe wires are shown in Fig. 2. As is usual for sheathed superconductors [15, 16] the resistance in normal state is practically that of sheating (thus its size depends on the length of the wire segment), whereas the resistive onset in entirely due to the superconducting core. It is observed that the magnetic field affects strongly the superconducting transition temperature T_c shifting it to the lower temperatures. Decrease of T_c and broadening of the transition is more pronounced for doped wires indicating that enhancement of flux pinning in magnetic nanoparticle doped MgB_2 wires was not achieved. Also, the T_c in zero applied field (determined from the $R(T, B)$ measurements) decreases quite rapidly (for about 1.4 K/wt.% of $CuFe_2O_4$) with the doping level (inset in Fig. 3). We obtained similar suppression of T_c (about 2 K/wt.%) in wire doped with Fe_3O_4 nanoparticles. Such strong suppression of T_c with small amount of dopand ($\leq$ 3 vol.%) is quite surprising, although quite common for bulk MgB_2 samples doped with Fe [8] or Fe-based magnetic nanoparticles [17]. The origin of this effect (often attributed to Fe [17]) has not been completely clarified [18], but it makes enhancement of $J_c(B)$ at temperatures $\geq$ 25 K in samples doped with $\geq$ 5 wt.% of such nanoparticles [4] highly unlikely.

The irreversibility field curves $B_{irr}(T)$, shown in Fig. 3, were obtained from the $R(T, B)$ measurements using the criteria of $R(T_{irr}, B_{irr})$ equals 10% of the resistance of the wire immediately above the transition [22]. In accordance with the lower T_c and weak flux pinning in doped wires, the values of $B_{irr}(T)$ of doped wires are smaller in the whole temperature range and increasing slower with decreasing temperature with respect to the undoped wire. The observed suppresion of $B_{irr}(T)$ upon doping (thus shrinkage of the vortex solid region) is not due to the suppression of T_c only: when the values of B_{irr} of our samples are plotted against reduced temperature $t = T_{irr}/T_{c0}$ (not shown) the values of $B_{irr}(t)$ in doped samples remain lower than those of undoped wire. $B_{irr}(T)$ of our wire doped with 5.3 wt.% Fe_3O_4 was quite similar to that of wire doped with 7.5 wt.% $CuFe_2O_4$.

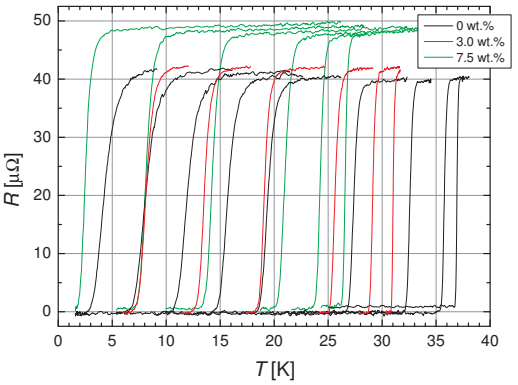

Fig. 2. Resistance versus temperature for undoped and $CuFe_2O_4$ nanoparticle doped MgB_2/Fe wires in applied magnetic fields (right to left): $B = 0, 1, 2, 4, 6, 8, 10, 12, 14, 16$ T.

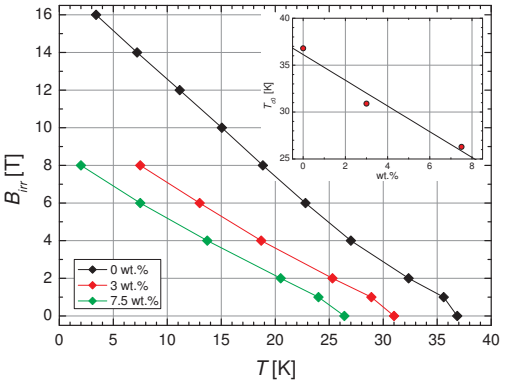

Fig. 3. Irreversibility field B_{irr} versus temperature T for undoped and doped MgB_2/Fe wires. Inset: Superconducting transition temperature in zero applied field T_{c0} versus doping level wt.%.

Magnetization versus applied magnetic field curves $M(H)$ were measured at various temperatures for undoped and 3 wt.% doped MgB_2 wire (Fig. 4). It is observed that, in spite of closely similar size, shape and mass of the samples [19], the vertical width ΔM of the $M(H)$ curves for the undoped MgB_2 sample are larger than for doped one at the same temperature. Considering that critical current density J_c is proportional to ΔM of the $M(H)$ curve, doped sample has smaller values of the J_c at all measured fields and temperatures. $M(H)$ curves for the undoped sample exhibit strong fluctuations at low temperature (5 K) and low field ($\leq$ 2 T) region. These fluctuations are usually associated with the thermomagnetic instability (fluxoid jumps) of flux lines penetrating into the superconductor and can be associated with large J_c [7, 14, 20]. Thus, the absence of jumps in $M(H)$ curve of doped sample is consistent with its low ΔM and J_{cm}.

We also note that doped sample shows small ferromagnetic $M(H)$ loop (inset in Fig. 4a)) just above its T_c (inset in Fig. 3). The maximum magnetization in the inset in Fig. 4a) would correspond to about 1.5 wt.% of $CuFe_2O_4$ nanoparticles in the sample, or more in line with XRD patterns to about 0.53 wt.% of Fe_2B nanoparticles [21]. This feature, althought important, is usually ignored [4] when discussing $M(H)$ loops and J_{cm} of samples doped with ferromagnetic nanoparticles at elevated temperatures.

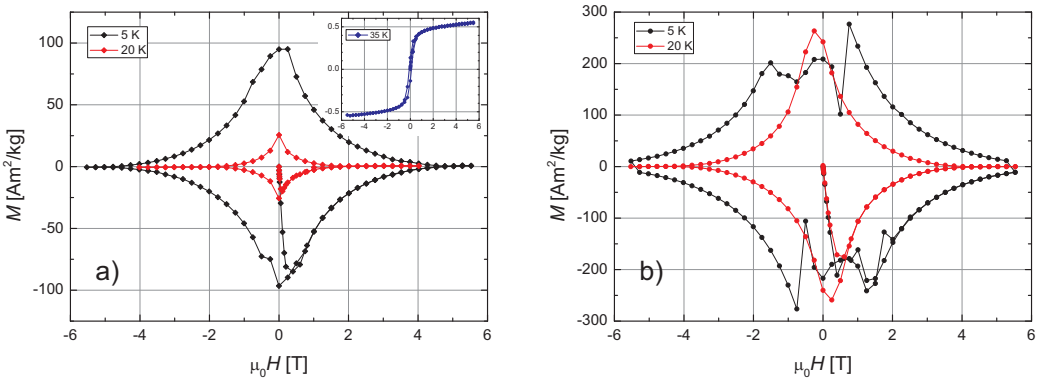

Fig. 4. a) Magnetic hysteresis loops for 3 wt.% doped MgB_2 sintered at 650°C. Inset: $M(H)$ curve above superconducting transition. b) Magnetic hysteresis loops for undoped MgB_2 sintered at 650°C.

The magnetic critical current densities J_{cm} (Fig. 5) were obatained from the measured magnetic hysteresis loops using the critical state model [10]. $J_{cm}(B)$ of the 3 wt.% doped sample showed worse performance with respect to undoped MgB_2 at all measured temperatures, both in their magnitude and field dependence. For further quantitative analysis we use only transport critical current densities J_{ct} because magnetic J_{cm}

are calculated using a model and they are sample size dependent and do not represent an accurate J_c of the MgB_2 wire [23]. In general, our magnetic and transport J_c are in a good qualitative agreement beacuse they both show the same trend of the change of J_c of the MgB_2 wires upon doping with $CuFe_2O_4$ nanoparticles.

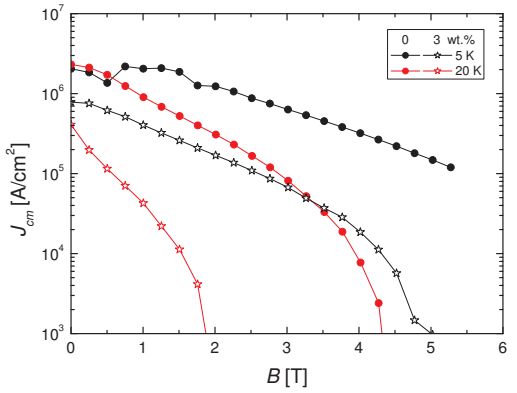

Fig. 5. Magnetic critical current density versus applied magnetic field for undoped and 3 wt.% doped MgB_2/Fe wires.

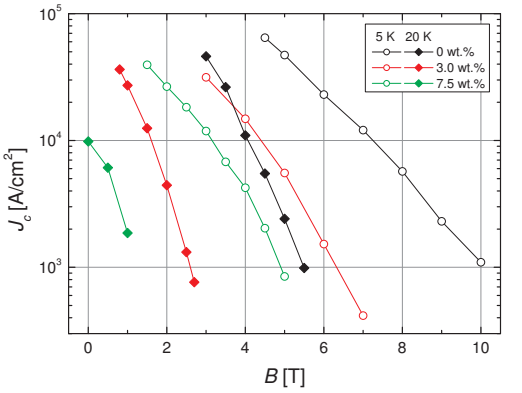

Fig. 6. Transport critical current density versus applied magnetic field for undoped and doped MgB_2/Fe wires.

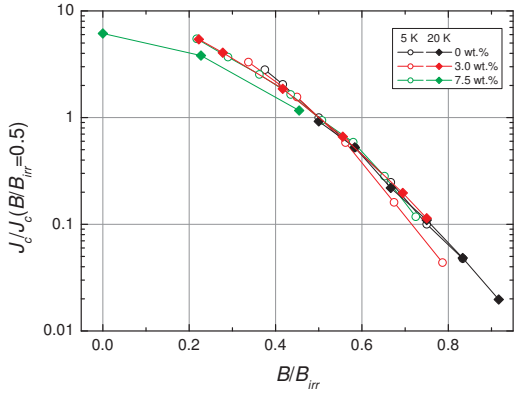

Fig. 7. Normalised transport critical current density versus normalised magnetic field for undoped and doped MgB_2/Fe wires.

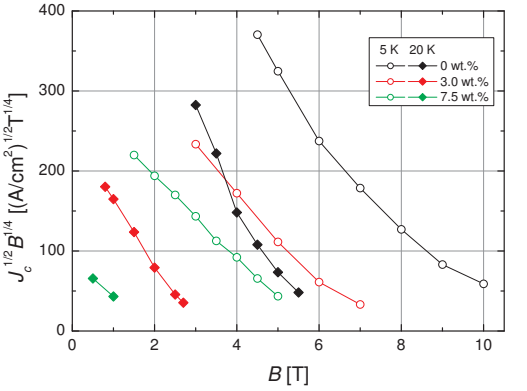

Fig. 8. Kramer's plots for undoped and doped MgB_2/Fe wires.

Transport critical current densities, deduced directly from the measured $V(I)$ curves, are shown in Fig. 6. As observed in Fig. 6, doping MgB_2 with $CuFe_2O_4$ nanoparticles causes deterioration of the $J_c(B)$ performance of the wires, in particular doped wires have considerably smaller values of the J_c and J_c decreases more rapidly with the increasing magnetic field than for undoped wire, both at high (20 K) and low (5 K) temperature. Fast decrease of J_c on increasing B is clear indication of weak flux pinning in MgB_2 samples. We note that also in ref. [4] (which reported strong enhancement of J_c in MgB_2 doped with Fe_3O_4 nanoparticles) the rate of decrease of J_c with B was larger in samples doped with Fe_3O_4 than that in nano-SiC doped samples at temperatures $\leq$ 25 K. Our preliminary results for wire doped with 5.3 wt.% Fe_3O_4 nanoparticles show strong deterioration of $J_c(B)$ performance similar to that observed for 7.5 wt.% doped wire in Fig. 6. The rates of suppression of T_c, $B_{irr}(T)$ and $J_c(B)$ in wires doped with $CuFe_2O_4$ and Fe_3O_4 particles, respectively, show that the magnetic effect prevails. This is similar to what was observed in MgB_2 wires doped with iron boride nanoparticles [10]. In order to assess the main pinning mechanism in doped wires we plot in Fig. 7 normalized J_c versus normalized field B/B_{irr}, for all samples and both temperatures (5 and 20 K). Overlap of the results for undoped and doped samples (small deviation for the 7.5 wt.% doped sample at 20 K is probably due to the proximity of the T_c) indicates that the main pinning mechanism in undoped and doped MgB_2 is the same. Volume pinning force densities $F_p = J_cB$ for doped samples (not shown) are

expectedly much lower than those for undoped sample. However, they reach maximum at normalised field $B/B_{irr} \approx 0.2$, which implies that the main flux pinning mechanism is grain boundary pinning [13, 16].

Kramer's plots $J_c^{1/2}B^{1/4}$ versus B are shown in Fig. 8. Linearity of Kramer's plots at high field region for doped samples also implies that the main pinning mechanism is grain boundary pinning. At highest fields Kramer's plots for undoped sample become rather curved indicating inhomogeneity of the sample. Suprisingly, according to Kramer's plots doped samples appear to be more homogeneous than udoped wire. This could, however, be associated with the lower maximum fields used for doped samples. The values of $B_{irr}(T)$ deduced from Kramer's plots agreed well with those in Fig. 3.

4. Conclusion

Electromagnetic properties ($B_{irr}(T)$, $J_c(B)$) of MgB_2 doped with superparamagnetic $CuFe_2O_4$ nanoparticles have been studied. Both magnetic and transport measurements showed strong deterioration of the superconducting properties of MgB_2 upon doping with $CuFe_2O_4$ nanoparticles. The preliminary results for Fe_3O_4 doped MgB_2 also showed suppression of $B_{irr}(T)$ and $J_c(B)$ performance. Besides, obtained results indicate that the pinning mechanism in $CuFe_2O_4$ doped MgB_2 and undoped MgB_2 is the same and that flux pinning accociated with the attractive magnetic force between vortices and magnetic nanoparticles was not achieved. Contrary to previous reports of Fe_3O_4 doping [4], our results clearly revealed deterioration of superconducting properties of MgB_2 upon doping with ferrite nanoparticles. A probable reason for this discrepancy is that in ref. [4] (like in other papers reporting enhanced flux pinning by magnetic particles) J_c was calculated from $M(H)$ loops only, which is not reliable [23, 19] (as shown recently for Fe_2B doped MgB_2 wires [10]). Indeed, different densities and microstructures/phases in samples doped with SiC and Fe_3O_4 particles in ref. [4] could have affected the resulting (magnetic) J_cs. We note, however, that our results do not prove that magnetic flux pinning does not exist in MgB_2 wires, all they show is that the employment of magnetic flux pinning in bulk MgB_2 samples is more complex than that in thin films [24].

References

[1] Vinod K, Abhilash Kumar R G, Syamaprasad U. Supercond Sci Technol **20** 2007 R1–R13.
[2] Yeoh W K, Horvat J, Kim J H, Dou S X. Improvement of vortex pinning in MgB_2 by doping. Hauppauge NY: Nova Science Pub. Inc.
[3] Collings E W, Sumption M D, Bhatia M, Susner M A, Bohnenstiehl S D. Supercond Sci Technol **21** 2008 103001 (14pp).
[4] Qu B, Sun X D, Li J-G, Xiu Z M, Liu S H, Xue C P. Supercond Sci Technol **22** 2009 015027(4pp).
[5] Snezhko A, Prozorov T, Prozorov R. Phys Rev B **71** 2005 024527 1–6.
[6] Cheng C, Zhao Y. Physica C **463–465** 2007 220–224.
[7] Awana V P S, Isobe M, Singh K P, Takayama-Muromachi E, Kishan H. Supercond Sci Technol **19** 2006 551–555
[8] Dou S X, Soltanian S, Zhao Y, Getin E, Chen Z, Shcherbakova O, Horvat J. Supercond Sci Technol **18** 2005 710–715.
[9] Kuroda T, Nakane T, Uematsu H, Kumakura K. Supercond Sci Technol **19** 2006 1152–1157.
[10] Novosel N, Pajić D, Mustapić M, Babić E, Shcherbakov A, Horvat J, Skoko Ž, Zadro K. J Phys Conf Ser **234** 2010 022027 1–7.
[11] This work is supported by Unity Through Knowledge Fund (Croatia) under project UKF 1B 01/07.
[12] Pajić D, Zadro K, Vanderberghe R E, Nedkov I. J Magn Magn Mater **281** 2004 353–363.
[13] Husnjak O, Babić E, Kušević I, Wang X L, Soltanian S, Dou S X. Solid State Commun **143** 2007 412–415.
[14] Singh K P, Awana V P S, Balamurugan S, Shahabuddin M, Singh H K, Husain M, Kishan H, Bauminger E R, Felner I. J Supercond Nov Magn **21** 2008 39–44.
[15] Babić E, Kušević I, Dou S X Liu H K, Hu Q Y. Phys Rev B **49** 1994 15312–15316.
[16] Kušević I, Babić E, Husnjak O, Soltanian S, Wang X L, Dou S X. Solid State Commun **132** 2004 761–765.
[17] Lue C S, Su T H, Xie B X, Chen S K, MacManus-Driscoll J L, Kuo Y K, Yang H D. Phys Rev B **73** 2006 214505 1–5.
[18] Bhasker Gahtori, Ratan Lal, Agarwal S K, Kuo Y K, Sivakumar K M, Hsu J K, Lin J Y, Ashok Rao, Chen S K, MacManus-Driscoll J L. Phys Rev B **75** 2007 184513 1–8.
[19] Horvat J, Soltanian S, Wang X L, Dou S X. Appl Phys Lett **84** 2004 3109–3111.
[20] Babić E, Miljanić Đ, Kušević, Marohnić Ž, Drobac Đ, Wang W L, Dou S X. Fizika A **10** 2001 87–94.
[21] Mustapić, Pajić D, Novosel N, Babić E, Zadro K, Cindrić M, Horvat J, Skoko Ž, Bijelić M, Shcherbakov A. Croat Chem Acta **83** 2010 275–282.
[22] Dou S X, Shcherbakova O, Yeoh W K, Kim J H, Soltanian S, Wang X L, Senatore C, Flukiger R, Dhalle M, Husnjak O, Babić E. Phys Rev Lett **98** 2007 097002 1–4.
[23] Horvat J, Yeoh W K, Kim J H, Dou S X. Supercond Sci Technol **21** 2008 065003 (6pp).
[24] Moshchalkov V V, Fritzsche J. Nanostructured superconductors. World Scientific, Singapore, 2011.